J. Biochem. 129, 513–520 (2001)

Characterization of the Flavoprotein Domain of gp91*phox* Which Has NADPH Diaphorase Activity

Chang-Hoon Han,* Yukio Nisimoto,†,[1] Sung-Haeng Lee,*,[2] Eugene T. Kim,*,[3] and J. David Lambeth*

**Department of Biochemistry, Emory Medical School, Atlanta, Georgia 30322, USA; and †Department of Biochemistry, Aichi Medical University, Nagakute, Aichi 480-1195*

Received December 7, 2000; accepted January 4, 2001

A series of truncated forms of gp91*phox* were expressed in *Escherichia coli* in which the N-terminal hydrophobic transmembrane region was replaced with a portion of the highly soluble bacterial protein thioredoxin. TRX-gp91*phox* (306–569), which contains the putative FAD and NADPH binding sites, showed weak NADPH-dependent NBT (nitroblue tetrazolium) reductase activity, whereas TRX-gp91*phox* (304–423) and TRX-gp91*phox* (424–569) were inactive. Activity saturated at about a 1:1 molar ratio of FAD to TRX-gp91*phox* (306–569), and showed the same K_m for NADPH as that for superoxide generating activity by the intact enzyme. Activity was not inhibited by superoxide dismutase, indicating that it was not mediated by superoxide, but was blocked by an inhibitor of the respiratory burst oxidase, diphenylene iodonium. In the presence of Rac1, the cytosolic regulatory protein p67*phox* stimulated the NBT reductase activity, but p47*phox* had no effect. Truncated p67*phox* containing the activation domain (residues 199–210) [C.-H. Han, J.R. Freeman, T. Lee, S.A. Motalebi, and J.D. Lambeth (1998) *J. Biol. Chem.* 273, 16663–16668] stimulated activity approximately 2-fold, whereas forms mutated or lacking this region failed to stimulate the activity. Our data indicate that: (i) TRX-gp91*phox* (306–569) contains binding sites for both pyridine and flavin nucleotides; (ii) this flavoprotein domain shows weak diaphorase activity; and (iii) the flavin-binding domain of gp91*phox* is the target of regulation by the activation domain of p67*phox*.

Key words: diaphorase activity, flavoprotein domain of gp91*phox*, NBT reductase activity.

Neutrophils and macrophages produce superoxide (O_2^-) and secondary reactive oxygen species (H_2O_2, HOCl) that participate in the killing of phagocytized microorganisms (*1–4*). Superoxide generation is catalyzed by a multicomponent enzyme, the respiratory burst oxidase or NADPH oxidase. The catalytic moiety is a plasma membrane–associated flavocytochrome, b_{558}, which is composed of two subunits, gp91*phox* and p22*phox* (*5–9*). The flavocytochrome is inactive in resting cells, but upon cell stimulation, the flavocytochrome is activated by assembly with the cytosolic regulatory proteins p47*phox*, p67*phox* (*10–13*), and Rac (Rac2 and/or Rac1) (*14–16*).

The large subunit of the flavocytochrome, gp91*phox* has a highly hydrophobic N-terminus that is predicted to contain 5–6 transmembrane helices (*17–19*) (Fig. 1). The flavocytochrome contains two hemes (*20–22*), which reside solely in gp91*phox* (*23*), as well as a single FAD (*21*, *24*, *25*). Various models (*22*, *23*) suggest that the heme groups both reside within the hydrophobic N-terminal half of the molecule, and specific histidines within this region have been suggested to be heme ligands. The relatively hydrophilic C-terminal half of gp91*phox* is homologous to several flavoprotein dehydrogenases, particularly in putative FAD and NADPH binding sequences (*20*, *26*, *27*) (Fig. 1), and is therefore predicted to form an independently folding flavoprotein domain. Direct binding of native FAD and FAD analogs to flavocytochrome b_{558} has been demonstrated by several groups (*21*, *25*, *26*). Localization of the FAD binding region is predicted from studies using plasma membranes from a Chronic Granulomatous Disease patient with a point mutation at His-338, which showed low FAD content in the plasma membrane and failed to produce superoxide (*28*). The location of the NADPH binding site is not well established. Although gp91*phox* contains regions homologous to known NADPH binding sites (Fig. 1, hash marks), direct binding of NADPH or $NADP^+$ has not been demonstrated. Different affinity labeling analogs of NADPH show binding to either gp91*phox* (*29*, *30*) or p67*phox* (*31–33*). The latter result has led to the suggestion that p67*phox* contains the binding site for pyridine nucleotide (or a portion thereof) and that activation might involve bringing this

[1] To whom correspondence should be addressed. Tel: +81-561-62-3311, Fax: +81-561-61-4056, E-mail: nisiio@amugw.aichi-med-u.ac.jp

Present addresses: [2] Department of Physiology and Biophysics, University of Texas Medical Branch at Galveston, Galveston, TX 77550, USA; [3] Department of Biochemical Science, Havard University, Cambridge, MA 02138, USA

Abbreviations: TRX, thioredoxin; *phox*, phagocyte oxidase; NBT, nitroblue tetrazolium; PCR, polymerase chain reaction; GST, glutathione S-transferase; IPTG, isopropyl-β-D-thiogalactopyranoside; GTPγS, guanosine 5′-(γ-thio)triphosphate; DMSO, dimethylsulfoxide; DPI, diphenylene iodonium; DTT, dithiothreitol; INT, iodonitrotetrazolium violet 2-(4-iodophenyl)-3-(4-nitrophenyl)-5-phenyltetrazolium chloride; DCPIP, 2,6-dichlorophenol indophenol.

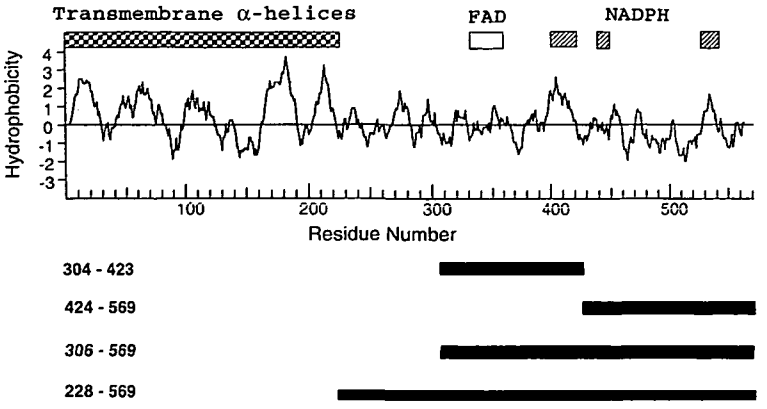

Fig. 1. **Domain structure of gp91*phox*.** Hydropathy of gp91*phox* as a function of residue number is shown. The extremely hydrophobic N-terminus of gp91*phox* is indicated by the checkered bar above the hydropathy plot, and this region is predicted to contain 5–6 transmembrane alpha helices. The putative FAD binding region (superior open bar) and regions implicated in NADPH binding (hatched bars) are indicated. A series of truncated forms indicated by the filled bars were constructed as N-terminal fusion proteins with thioredoxin (TRX).

binding site into juxtaposition with the flavin moiety on the flavocytochrome (*31–33*).

Individual roles for the cytosolic regulatory proteins in activating the NADPH oxidase have been proposed in recent studies. p47*phox* functions as a regulated adapter protein in a cell-free system; while it is not essential for cell-free NADPH oxidase activity, it increases the affinity of p67*phox* and Rac1 by about 2 orders of magnitude (*34, 35*). Both Rac and p47*phox* provide binding sites for p67*phox*, and Rac may function similarly to p47*phox* in binding and anchoring p67*phox* (*i.e.*, both may be regulated adapter proteins). We have proposed that it is p67*phox* that is the direct regulator of electron transfer within the flavocytochrome. An "activation domain" localized within amino acid residues 199–210 in p67*phox* is essential for cell-free NADPH oxidase activity (*36*), and a point mutation at residue 204 eliminates NADPH oxidase activity without affecting either the binding of p67*phox* to p47*phox* or Rac, or the assembly of the mutant p67*phox* in the NADPH oxidase complex (*36*). The target for this activation domain on p67*phox* is unknown, but we hypothesize that it is localized within the flavoprotein domain of the flavocytochrome (vide infra).

In this study, we have investigated the putative flavoprotein domain of gp91*phox*. The hydrophobic transmembrane heme-containing domain was eliminated and replaced by a highly soluble portion of bacterial thioredoxin. Using TRX-gp91*phox* (306–569), which is predicted to contain both FAD and NADPH binding sites, a weak NADPH diaphorase activity was detected and investigated. Our results indicate that this domain contains both the NADPH and FAD binding sites. In addition, the flavoprotein domain responds to regulation by p67*phox* and Rac, indicating the presence of interaction regions for one or both of these factors.

MATERIALS AND METHODS

Truncation Mutations—A series of truncated gp91*phox* clones was obtained by PCR using gp91*phox* DNA cloned in the pGEX-2T plasmid (Pharmacia Biotech) as the template. The forward primers (CGT**GGATCC**CGTGGGCAGACCGCAGAGAGT for 228–569, CGT**GGATCC**CCTTTCAAAACCATCGACCTA for 304–423, CGT**GGATCC**TGGTACAAATATTGCAATAAC for 424–569, and CGT**GGATCC**AAAACCATCGAGCTACAGATG for 306–569) were designed to introduce a *Bam*HI site (shown in boldface). The reverse primers (CGT**AAGCTT**TTAGACTGACTTGAGAATGGATGC for 304–423, CGT**AAGCTT**TTAGAAGTTTTCCTTGTTGAAAAT for 228–569, 306–569, and 424–569) were designed to introduce a *Hin*dIII site (shown in boldface) and a stop codon (underlined). These PCR products were purified with a PCR purification kit (Qiagen), and digested with *Bam*HI and *Hin*dIII (GIBCO BRL). The digested samples were purified by 1% agarose gel electrophoresis, and extracted from agar by a Gel extraction kit (Qiagen). The purified DNA fragments were ligated into the *Bam*HI and *Hin*dIII sites of pET-32a(+) vector (Novagen), and then transformed into BL21 (DE3). Transformants were selected from LB/Ampicillin plates, and plasmids were isolated from 2 ml cultures of transformants as described previously (*34*). The plasmids were digested with *Bam*HI and *Hin*dIII, and were separated on 1% agarose to confirm the presence of the insert. The clones were sequenced to rule out unexpected mutations and to confirm the truncations.

Expression and Purification of Recombinant Proteins—Recombinant proteins p47*phox* and wild-type p67*phox* were expressed in insect cells (sf9 cell) and purified according to Uhlinger *et al.* (*37, 38*). Rac1 cDNA cloned in pGEX-2T was expressed in DH5a cells as a GST fusion form, purified by binding to glutathione-Sepharose (Pharmacia Biotech.), and cleaved with thrombin (Sigma) (*39*). Truncated and point mutated forms of p67*phox*-GST fusions were expressed and purified as above except that thrombin was not used and the proteins were eluted with 100 mM glutathione (Sigma) (*36*).

For preparation of TRX-tgp91*phox* fusion proteins, *E. coli* were grown at 37°C in LB media (1 liter) to an A_{550} of 0.4. IPTG (Sigma) (1 mM) was added and the cells were shaken at 37°C for 4 h. Except for the 424–569 form, the truncated forms of gp91*phox* were initially insoluble. These were solubilized and renatured according to a modification of the method of Gentz *et al.* (*40*). Cells were pelleted by centrifuging at 4,500 ×*g* for 15 min, resuspended in 6 M guanidine HCl (GIBCO BRL), pH 7.8, 50 mM Tris-HCl, 500 mM NaCl, and incubated on ice for 1 h. Insoluble material was removed by centifugation at 30,000 ×*g* for 20 min. The supernatant was applied to a nickel chelate affinity resin (ProBond, Invitrogen), which was washed 3 times with several volumes of wash buffer (8 M urea, 500 mM NaCl, 50 mM Tris-HCl, pH 7.8). The protein was eluted with the same buffer containing 500 mM imidazole (Sigma). Dithiothreitol (DTT, Sigma) (2 mM) was added and samples were dialyzed for 5 h against a sequential series of buffers con-

taining 2 mM DTT plus 1 M urea, 0.2 M urea, and then no urea. DTT was removed after the final step by dialysis against 500 mM NaCl, 50 mM Tris-HCl, pH 7.8. Protein concentration was determined according to Bradford (*41*) and samples were stored at −80°C.

NBT Reductase Activity Assay—NBT reductase activity was determined using a Thermomax Kinetic Microplate reader (Molecular Devices, Menlo Park, CA). Expressed forms of gp91*phox* were preincubated in most experiments with an equimolar ratio of FAD (Sigma) (or, in the case of FAD titration, with varying ratios of FAD/protein) for 16 h at 4°C before use. The incubation contained 4 μM of FAD-preloaded TRX-gp91*phox* (306–569) and combinations of cytosolic regulatory proteins [4.8 μM p67*phox*, 4.2 μM p47*phox*, and/or 5.4 μM Rac1, which had been preloaded with GTPγS (Sigma) (*39*), all in a 50 μl volume of assay buffer (100 mM KCl, 3 mM NaCl, 4 mM $MgCl_2$, 1 mM EGTA, and 10 mM PIPES, pH 7.0). Diphenylene iodonium (DPI, Fluka) was prepared as a 1 mM stock solution in DMSO, and working solutions were prepared by dilution into assay buffer. An extinction coefficient of 15.1 mM^{-1} cm^{-1} at 264 nm was used to determine concentration (*42*). Three 10 μl aliquots of each reaction mixture were transferred to 96-well assay plates and preincubated for 5 min at 25°C. Assay buffer (250 μl) containing 200 μM NADPH (Sigma) and 200 μM NBT (Sigma) was added to each well. NBT reduction was quantified by monitoring absorbance at 595 nm using an extinction coefficient of 12.6 mM^{-1} cm^{-1} at 595 nm (*43*).

Calculation of Dissociation Constants (K_d)—The K_d value for the binding of FAD to truncated gp91*phox* (306–569) was obtained using the following equation, modified from (*44*),

$$\Delta v = \Delta V_{max} [((K_d + L_T + E_T) - ((K_d + L_T + E_T)^2 - 4L_T E_T)^{1/2})/2E_T] \quad (1)$$

where Δv is the increase in the initial rate produced by a given concentration of FAD, ΔV_{max} is the maximal velocity change at infinite (extrapolated) FAD, K_d is the dissociation constant, L_T is the concentration of FAD, and E_T is the total concentration of truncated gp91*phox* (306–569). Sigma plot was used to generate a nonlinear least squares fit of the data, solving for K_d and ΔV_{max}, constraining the fit to the actual concentration of TRX-gp91*phox* (306–569).

RESULTS

Expression of TRX-Fusion Forms of Truncated gp91phox—The expression strategy was designed based on the idea that the C-terminal half of gp91*phox* is relatively hydrophilic, and that this domain will fold independently. We initially constructed a series of truncated mutants as N-terminal GST fusion proteins and His_6 fusions. Those were: gp91*phox* (190–569), (228–569), (304–569), (424–569), and (304–423). All constructs except for gp91*phox* (190–569), which contains a large hydrophobic segment, were expressed at high levels in *E. coli*. However, neither GST nor His_6 fusion forms were soluble, and denaturation/renaturation methods (vide infra) failed to generate soluble products.

In contrast, the thioredoxin fused forms of truncated gp91*phox* [TRX-gp91*phox* (304–423), TRX-gp91*phox* (424–569), and TRX-gp91*phox* (306–569)] were successfully expressed and readily solubilized using an urea unfolding/refolding method (Fig. 2). TRX-gp91*phox* (228–569) was also expressed, but it was not possible to solubilize this form. The largest form of soluble protein, TRX-gp91*phox* (306–569), is predicted based on sequence homology to contain binding sites for both FAD and NADPH (Fig. 1). The highly soluble TRX domain reportedly improves the solubility of proteins to which it is fused (*45*), and the vector also encodes a hexa histidine that allows purification under denaturing conditions on a Ni^{2+}-chelate affinity matrix. The proteins were purified under denaturing conditions, since TRX-gp91*phox* (304–423) and TRX-gp91*phox* (306–569) in particular were poorly soluble and not retained on a His_6 matrix under non-denaturing conditions, despite the fact that they were highly expressed. In contrast, TRX-gp91*phox* (424–569) was highly expressed and showed good recovery in both the presence and absence of 8 M urea. All purified proteins corresponded in size to their predicted molecular weights on SDS-PAGE (Fig. 2).

Physical Properties of Expressed Proteins—Although the flavoprotein domains of gp91*phox* [TRX-gp91*phox* (304–423), TRX-gp91*phox* (424–569), and TRX-gp91*phox* (306–569)] were obtained in "soluble" forms showing no apparent turbidity, they appeared to be aggregates of 4 or more monomers. The proteins preincubated with 0.1 mM FAD were chromatographed on a Sephacryl S-300 column equilibrated with 20 mM Tris-HCl buffer, pH 7.4, containing 50 mM NaCl. All proteins eluted at or near the void volume (MW ≥ 200 kDa). On SDS-PAGE in the absence of DTT, they migrated as large molecular size (apparent size greater than 106 kDa) smeared bands (data not shown). However, when the proteins were treated with SDS sample buffer containing 80 mM DTT, they showed the correct predicted molecular masses of 32, 34.5, and 48 kDa, respectively, on a 12% SDS-PAGE gel (Fig. 2). These results imply that the recombinant gp91*phox* exists in a polymerized

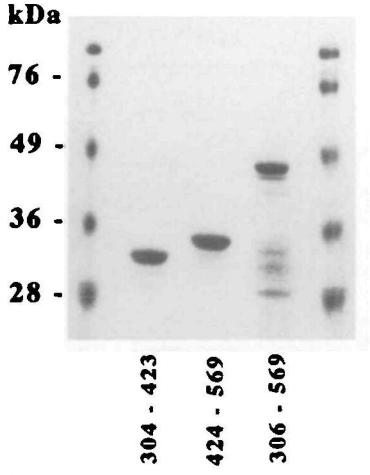

Fig. 2. **SDS-PAGE of the expressed TRX-fusion forms of truncated gp91*phox*.** The TRX-$(His)_6$-fusion forms of truncated gp91*phox* were expressed in *E. coli* and purified on a Ni^{2+}-chelating column as described in "MATERIALS AND METHODS." The purified proteins were subjected to SDS-PAGE in a 12% (w/v) polyacrylamide gel, and visualized by Coomassie-Blue staining. The apparent molecular sizes of the TRX fusion forms of gp91*phox* (304–423), gp91*phox* (424–569), and gp91*phox* (306–569) were 32, 34.5, and 48 kDa respectively.

state in ordinary buffer even in the presence of detergent unless a reducing agent is added, suggesting that there might be intermolecular disulfide bridges. However, DTT interfered with the diaphorase assays (below) and was therefore not included.

NADPH-Dependent Diaphorase Activities of TRX-gp91-phox (306–569)—Table I shows the activity of TRX-gp91-*phox* (306–569) reconstituted with excess FAD in the presence or absence of cytosolic factors using various artificial electron acceptors. NBT reduction produced the highest activity among several electron acceptors investigated. Interestingly, both NBT and INT reduction rates were increased by the addition of the cytosolic regulatory proteins p67-*phox*, p47*phox*, and Rac1 (GTPγS). The maximal rate of NBT reduction at saturating FAD concentration was low, about 4 electrons/min/molecule of protein. The NBT reductase activity of the shorter gp91*phox* fragments was also investigated under the same conditions in the presence and absence of NADPH. The longest fusion protein, TRX-gp91-*phox* (306–569), showed NADPH-dependent activity (Fig. 3) as above. However, the shorter forms, TRX-gp91*phox* (304–423) and TRX-gp91*phox* (424–569), showed only background NBT reductase activity (Fig. 3). The K_m for NADPH in the longest protein was determined to be 45 μM (Fig. 4) in the absence of cytosolic factors. This value is similar to the K_m for NADPH (~50 μM) observed in the intact phagocyte NADPH oxidase (*30*). TRX-gp91*phox* (306–569) shows a specificity for NADPH over NADH due to K_m effects but not to V_{max}. The K_m and V_{max} values were not affected by superoxide dismutase added to the assay medium, indicating that NBT reduction is not brought about by superoxide anion.

TABLE I. **Diaphorase activities of TRX-gp91*phox* (306–569) in the presence and absence of cytosolic factors.**

Electron acceptor	Rate (nmol reduced/min/mg of tgp91*phox*)	
	(−)	(+)
Cytochrome *c*	6.51 ± 0.88	8.85 ± 0.22
NBT	10.23 ± 0.65	19.91 ± 1.70
INT	1.70 ± 0.27	6.78 ± 0.26
Ferricyanide	0	0
DCPIP	0	0

The assay for NADPH diaphorase activity was carried out as described in "MATERIALS AND METHODS." The truncated gp91*phox* was preincubated with (+) or without (−) cytosolic factors. The assay buffer contained 0.2 mM of each electron acceptor and the reaction was started by adding 0.2 mM NADPH. The molar extinction coefficients used for cytochrome *c*, NBT, INT, ferricyanide and DCPIP were 21.1 at 550 nm (*60*), 12.6 at 595 nm (*43*), 11.0 at 500 nm (*52*), 1.01 at 420 nm (*61*), and 21.0 mM^{-1} cm^{-1} at 600 nm (*62*), respectively. Values shown are the average ± SEM of three determinations. For NBT reduction, it was assumed for convenience that the extinction change represented a complete 4-electron reduction, although it should be recognized that this need not be the case for this complicated electron acceptor.

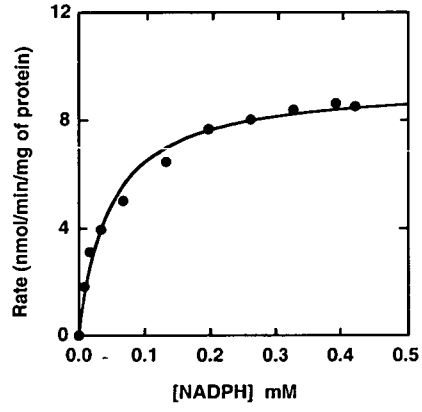

Fig. 4. **NADPH concentration dependence of the NBT reductase activity of TRX-gp91*phox* (306–569).** The assay conditions were as described in the legend to Fig. 3, except that the reaction was initiated by the addition of 10 μl of the activation mixture to a 240 μl solution containing 0.2 mM of NBT and the indicated concentrations of NADPH.

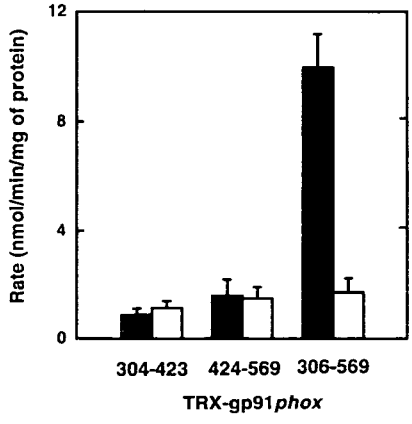

Fig. 3. **NADPH-dependent NBT reductase activity of TRX-gp91*phox*.** Each form of TRX-gp91*phox* was preincubated with an equimolar amount of FAD for 16 h at 4°C as described in "MATERIALS AND METHODS." NBT reductase activity was measured using 4 μM of each protein in a volume of 50 μl. The reaction was initiated by the addition of 10 μl of this mixture to a 240 μl solution cotaining 0.2 mM of NBT in the presence (filled bars) or absence (open bars) of 0.2 mM NADPH. Error bars show the standard error of the mean (n = 3).

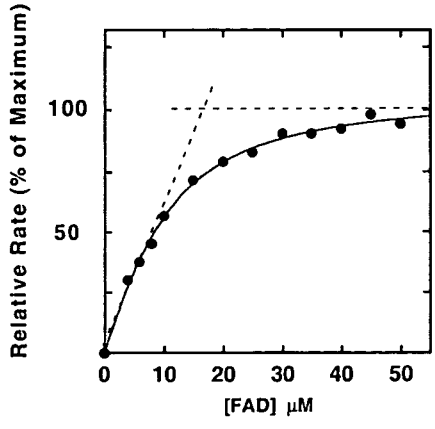

Fig. 5. **FAD concentration dependence of the NBT reductase activity of TRX-gp91phox (306–569).** TRX-gp91*phox* (306–569) (20 μM) was preincubated with varying concentrations of FAD for 16 h at 4°C as indicated. NBT reduction of the FAD-reconstituted preparations was measured as described in "MATERIALS AND METHODS" using 4 μM TRX-gp91*phox* (306–569) in a 50 μl volume. The reaction was initiated by the addition of 10 μl of this mixture to a 240 μl of reaction mixture containing 0.2 mM each of NADPH and NBT.

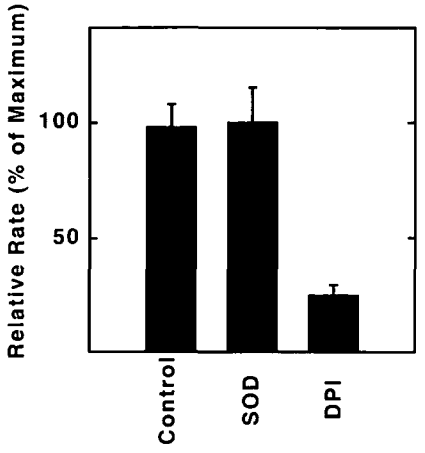

Fig. 6. **Inhibition of the NBT reductase activity of TRX-gp91*phox* (306–569).** NBT reduction was measured using 4 μM of FAD-preloaded TRX-gp91*phox* (306–569) in a 50 μl volume in the presence or absence of either 10 units superoxide dismutase (SOD) or 10 μM diphenylene iodonium (DPI). The reaction was initiated by the addition of 10 μl of this mixture to 240 μl of reaction buffer containing 0.2 mM each of NADPH and NBT. Error bars show the standard error of the mean (n = 3).

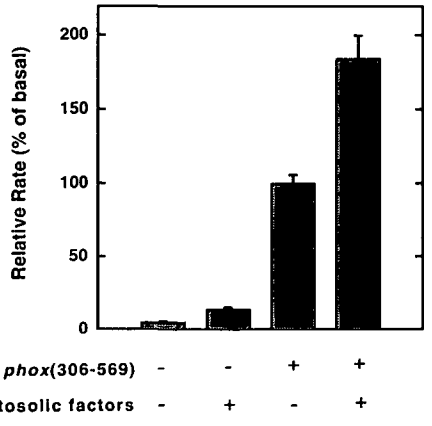

Fig. 7. **Effects of cytosolic factors on the NBT reductase activity of TRX-gp91phox (306–569).** TRX-gp91*phox* (306–569) (20 μM) was preincubated with 20 μM of FAD for 16 h at 4°C before use. NBT reduction was measured using 4 μM of FAD preloaded TRX-gp91*phox* (306–569) in a volume of 50 μl in the presence or absence of the cytosolic factors (4.8 μM p67*phox*, 4.2 μM p47*phox*, 5.4 μM Rac1). The reaction was initiated by the addition of 10 μl of this mixture to a 240 μl solution containing NADPH (0.2 mM) and NBT (0.2 mM). Error bars show the standard error of the mean (n = 3).

FAD-Dependence of NADPH-NBT Reductase Activity of TRX-gp91phox (306–569)—The activity was dependent on FAD (Fig. 5), and increased more or less linearly up to a FAD/protein ratio of approximately 0.8:1, approaching saturation thereafter. Curve fitting revealed an apparent K_d of 740 nM for the binding of a single FAD to the protein. The relatively tight binding of FAD and the "normal" K_m for NADPH suggest that the flavoprotein domain of TRX-gp91*phox* (306–569) achieves a more-or-less native structure following expression and renaturation. The observation of a stoichiometry of FAD binding to protein near 1:1 suggests that despite its polymeric state, most of the flavoprotein domain is in an active form.

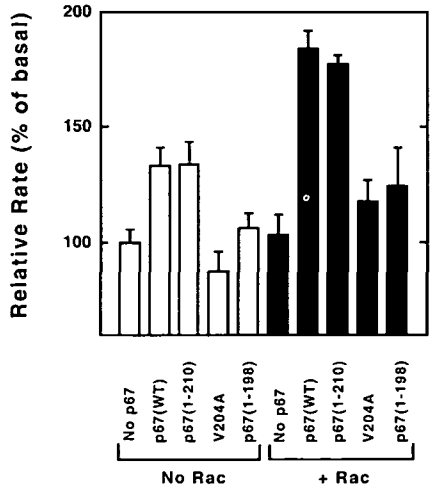

Fig. 8. **Effects of mutation/truncation in the activation domain of p67*phox* on the NBT reductase activity of TRX-gp91*phox* (306–569).** The assay conditions were as described in the legend to Fig. 7, except that mutant forms of p67*phox* (4.8 μM) were used with (filled bars) or without (open bars) Rac1 (5.4 μM). Error bars show the standard error of the mean (n = 3).

Inhibition of NADPH-NBT Reductase Activity of TRX-gp91phox (306–569)—NBT reductase activity of TRX-gp91-*phox* (306–569) was not inhibited by superoxide dismutase (Fig. 6), indicating that NBT reduction is not mediated by superoxide. Thus, it seems likely that NBT accepts electrons directly from the reduced FAD. DPI, a known inhibitor of NADPH-dependent superoxide generation by the intact phagocyte oxidase (*44*), blocked NADPH-dependent NBT reduction (approximately 70%). As mentioned above, since the truncate gp91*phox* is very aggregative in the assay medium, DPI does not appear to be stringently bound to a flavin-occupied catalytic center, resulting in its incomplete inhibitory effect.

Effects of Cytosolic Regulatory Factors on the NBT Reductase Activity of TRX-gp91phox (306–569)—As shown in Table I and Fig. 7, the NBT reductase activity of TRX-gp91 (306–569) increased nearly 2-fold in the presence of the cytosolic regulatory proteins p47*phox*, p67*phox*, and Rac1 (GTPγS). Activity was dependent upon TRX-gp91*phox* (306–569), and cytosolic factors alone showed almost no activity. Thus, one or more cytosolic regulatory proteins can stimulate the NBT reductase activity of TRX-gp91*phox* (306–569). To explore further the requirement for cytosolic factors, the activity was measured in the presence of combinations of cytosolic factors. Elimination of p47*phox* had no effect on NBT reductase activity (not shown). As shown in Fig. 8, p67*phox* stimulated the activity in the absence of other cytosolic factors. Rac alone had little or no stimulatory effect, but increased the magnitude of the stimulation by p67*phox* (Fig. 8).

The effect of the "activation domain" of p67*phox* on NBT reductase activity of the flavoprotein domain was also investigated. p67*phox* (1–210), which contains the activation domain, stimulated activity as well as the wild type p67*phox*. However, p67*phox* (1–198), which lacks the activation domain, was ineffective. Similarly, p67*phox* (V204A), which contains a point mutation in the activation domain and is completely inactive in the cell-free NADPH-oxidase

assay (*36*), is also ineffective in stimulating diaphorase activity (Fig. 8).

DISCUSSION

In the previous paper (*20*), the concentration of FAD in the membranes of resting neutrophils was reported to be very similar to that in activated cells, indicating that the ratio of FAD/heme = 1:2 remained fairly constant. In addition, in the cell-free NADPH oxidase system, flavinated flavocytochrome b_{558} showed almost the same turnover number of superoxide generation as that observed in activated membranes (*20*, *26*). On the other hand, it has been demonstrated that p67*phox* contains the NADPH-binding site of NADPH oxidase that is essential for catalytic activity. According to these reports, it is suggested that the active site of the oxidase is distributed between p67*phox* and gp91*phox* that are only brought together when the enzyme is activated (*31–33*). The recombinant p67*phox* we prepared, however, contained little or no FAD and its diaphorase activity was very low in the presence and absence of flavin, suggesting that the protein is unlikely to have the catalytic properties of NADPH dehydrogenase. In view of these results, we support the idea that flavocytochrome b_{558} is only the redox component, possessing NADPH, FAD and 2 heme-binding domains, and that p67*phox* regulates electron flow between the redox centers in the flavocytochrome.

Based on previous models, the globular portion of the β subunit of flavocytochrome b_{558} is largely exposed to the solvent and accessible to NADPH from the cytoplasm (*46*). Several flavin-dependent reductases possess a β-stranded barrel structure for FAD binding (*47, 48*). The sequence alignment of the FAD binding domain of gp91*phox* and the ferredoxin-$NADP^+$ reductase family has shown that amino acid residues 279–400 of gp91*phox* are homologous to a general FAD binding structure (*28*). The HPFT motif (residues 338–341) in this structure is predicted to interact directly with FAD in the flavocytochrome b_{558} model (*46*), and is conserved in human, porcine, and mouse gp91*phox* (*49*, *50*). The aim of this study was to express a flavoprotein-homology domain of flavocytochrome b_{558} lacking the transmembrane heme-binding regions, and to investigate its catalytic properties. gp91*phox* (306–569) includes most of the predicted β-stranded barrel structure, including the HPFT motif, and also contains regions that are predicted to form the NADPH binding site (Fig. 1). This structure was successfully expressed as a TRX fusion protein and showed low catalytic activity (NBT and INT reductase activities). The low diaphorase activity may either be an intrinsic property of the flavoprotein domain, or may indicate that the expressed flavoprotein is catalytically inefficient due to its cross-linked nature or the absence of an appropriate conformation. In a previous study, the anaerobic rate of FAD reduction was less than 1% of the aerobic rate (*51*), and the authors proposed that oxygen induces a conformation that favors flavin reduction. Since there is no heme in TRX-gp91*phox* (306–569), such conformational regulation may not be possible. The intact flavocytochrome also catalyzes a low rate of INT reduction (*52*), but this rate is still approximately 100–200-fold higher than that seen in the present study, suggesting either a less efficient electron transfer in the expressed flavoprotein domain, or additional electron transfer mechanisms in the intact cytochrome. The low activity may make this preparation of limited utility for mechanistic studies, but the model system appears to be adequate for drawing a number of important conclusions.

The diaphorase activity of TRX-gp91*phox* (306–569) was found to be dependent upon FAD, which showed a relatively lower binding affinity (K_d = 740 nM) compared with 50 nM for the native enzyme (*24*). The expressed domain also showed a K_m for NADPH of about 50 μM, the same value seen for the NADPH-superoxide generating activity of the intact respiratory burst oxidase. These data indicate that the expressed, renatured protein forms a reasonably intact structure, sufficient to bind both NADPH and FAD and to catalyze a diaphorase activity, albeit at a very low rate. These data demonstrate unequivocally that this domain contains binding sites for both an NADPH and a FAD. Although it is possible that p67*phox* also contains a binding site for NADPH, as was recently proposed (*31–33*), these data do not support the involvement of such a site in catalysis.

Importantly, these studies also reveal that the flavoprotein domain is the target of regulation by p67*phox*. Previously, we showed that an activation domain in p67*phox* (residues 199–210) is essential for NADPH-oxidase activation in a cell-free system (*36*). Truncated forms of p67*phox* lacking this region or a form containing a single mutation at residue 204 showed no ability to activate the oxidase, despite the fact that these forms bound normally to oxidase components and assembled normally as part of the oxidase complex under cell-free activation conditions. As shown in Fig. 8, these same alterations in the activation domain eliminated the ability of p67*phox* to activate the NBT-reductase activity of the flavoprotein domain. These data indicate that the target of the activation domain of p67*phox* resides within the flavoprotein domain of gp91*phox*. These data provide a physical explanation for the data indicating that the activation domain of p67*phox* controls the reduction of FAD by NADPH (*53*). Interestingly, this study shows that p67*phox* has little or no effect on NADPH binding, but the data are most consistent with the regulation of electron/hydride transfer from NADPH to FAD.

These studies fail to provide evidence for an effect of p47*phox* on regulation at the level of the flavoprotein domain. We have previously shown that p47*phox* is not essential for NADPH-dependent superoxide generation by the intact respiratory burst oxidase under cell-free conditions (*34*). Its role was proposed to be to ect as a regulated adapter protein, since its effect was to enhance the affinity of p67*phox* and Rac by up to 100-fold. To our knowledge, p47*phox* binding to the flavoprotein domain has not been directly demonstrated (*54*, *55*), although controversial evidence has implicated the C-terminus of gp91*phox* in such an interaction (*56*). Binding sites for p47*phox* on both p22*phox* and the N-terminus of gp91*phox* (residues 86–102, not present in the flavoprotein domain) have been documented (*57*), and may be sufficient for the docking of this cytosolic component. Although Rac does not directly activate the flavoprotein domain, a role for Rac is implied by the present studies, since Rac enhances the effect of p67*phox*. Direct binding of Rac to p67*phox* *via* the "effector region" on Rac (residues 26–45) has been demonstrated (*58*), and Rac is known to bind to the plasma membrane through its C-terminus (*39*). A third region on Rac, the insert region (residues 124–135), is essential for optimal

activity, and is involved in protein–protein interactions within the assembled oxidase (*58, 59*); this region has been proposed to bind to the cytochrome, although this has not yet been demonstrated directly. Rac may act synergistically with p67*phox* in activating the diaphorase activity of the flavoprotein domain either by binding to p67*phox*, producing an active conformation, or by binding simultaneously to both p67*phox* and the flavoprotein domain of gp91*phox*. The present studies do not distinguish between these possibilities, but indicate that Rac somehow synergizes with p67*phox* to activate the flavoprotein domain of gp91*phox*. The ability of p67*phox* to activate NBT reductase activity in the absence of Rac, however, indicates that p67*phox* must interact directly with the flavoprotein domain, and that it is likely to be the primary regulatory element in this complex and elegant system.

REFERENCES

1. Joseph, G. and Pick, E. (1995) "Peptide walking" is a novel method for mapping functional domains. Its application to the Rac1-dependent activation of NADPH oxidase. *J. Biol. Chem.* **270**, 29079–29082
2. Clark, R.A. (1990) The human neutrophil respiratory burst oxidase. *J. Infect. Dis.* **161**, 1140–1147
3. Segal, A.W. and Abo, A. (1993) The biochemical basis of the NADPH oxidase of phagocytes. *Trends Biochem. Sci.* **18**, 43–47
4. Chanock, S., El Benna, J., Smith, R., and Babior, B. (1994) The respiratory burst oxidase. *J. Biol. Chem.* **269**, 24519–24522
5. Nakamura, M., Sendo, S., van Zweiten, R., Koga, T., Roos, D., and Kanegasaki, S. (1988) Immunocytochemical discovery of the 22- to 23-Kd subunit of cytochrome b_{558} at the surface of human peripheral phagocytes. *Blood* **72**, 1550–1552
6. Parkos, C.A., Dinauer, M.C., Walker, L.E., Allen, R.A., Jeasaitis, A.J., and Orkin, S.H. (1988) Primary structure and unique expression of the 22-kilodalton light chain of human neutrophil cytochrome b. *Proc. Natl. Acad. Sci. USA* **85**, 3319–3323
7. Segal, A.W. (1987) Absence of both cytochrome b_{-245} subunits from neutrophils in X-linked chronic granulomatous disease. *Nature* **326**, 88–91
8. Rotrosen, D., Kleinberg, M.E., Nunoi, H., Leto, T., Gallin, J.I., and Malech, H.L. (1990) Evidence for a functional cytoplasmic domain of phagocyte oxidase cytochrome b_{558}. *J. Biol. Chem.* **265**, 8745–8750
9. Imajoh-Ohmi, S., Tokita, K., Ochiai, H., Nakamura, M., and Kanegasaki, S. (1992) Topology of cytochrome b_{558} in neutrophil membrane analyzed by anti-peptide antibodies and proteolysis. *J. Biol. Chem.* **267**, 180–184
10. Clark, R.A.,Volpp, B.D., Leidal, K.G., and Nauseef, W.M. (1990) Two cytosolic components of the human neutrophil respiratory burst oxidase translocate to the plasma membrane during cell activation. *J. Clin. Invest.* **85**, 714–721
11. Dinauer, M.C., Pierce, E.A., Bruns, G.A.P., Curnutte, J.T., and Orkin, S.H. (1990) Human neutrophil cytochrome b light chain (p22*phox*). Gene structure, chromosomal location, and mutations in cytochrome-negative autosomal recessive chronic granulomatous disease. *J. Clin. Invest.* **86**, 1729–1737
12. Heyworth, P.G., Curnutte, J.T., Nauseef, W.M., Volpp, B.D., Pearson, D.W., Rosen, H., and Clark, R.A. (1991) Neutrophil nicotinamide adenine dinucleotide phosphate oxidase assembly. Translocation of p47*phox* and p67*phox* requires interaction between p47*phox* and cytochrome b_{558}. *J. Clin. Invest.* **87**, 352–356
13. Tyagi, S.R., Neckelmann, N., Uhlinger, D.J., Burnham, D.N., and Lambeth, J.D. (1992) Cell-free translocation of recombinant p47*phox*, a component of the neutrophil NADPH oxidase: Effects of guanosine 5′-O-(3-thiotriphosphate), diacylglycerol and anionic amphiphile. *Biochemistry* **31**, 2765–2774
14. Quinn, M.T., Evans, T., Loetterle, L.R., Jesaitis, A.J., and Bokoch, G.M. (1993) Translocation of Rac correlates with NADPH oxidase activation. Evidence for equimolar translocation of oxidase components. *J. Biol. Chem.* **268**, 20983–20987
15. Heyworth, P.G., Bohl, B.P., Bokoch, G.M., and Curnutte, J.T. (1994) Rac translocates independently of the neutrophil NADPH oxidase components p47*phox* and p67*phox*. Evidence for its interaction with flavocytochrome b_{558}. *J. Biol. Chem.* **269**, 30749–30752
16. Dorseuil, O., Quinn, M.T., and Bokoch, G.M. (1995) Dissociation of Rac translocation from p47*phox*/p67*phox* movements in human neutrophils by tyrosine kinase inhibitors. *J. Leukocyte Biol.* **58**, 108–113
17. Royer-Pokora, B., Kunkel, L.M., Monaco, A.P., Goff, S.C., Newburger, P.E., Baehner, R.L., Cole, F.S., Curnutte, J.T., and Orkin, S.H. (1986) Cloning the gene for an inherited human disorder, chronic granulomatous disease, on the basis of its chromosomal location. *Nature* **322**, 32–38
18. Dinauer, M.C., Orkin, S.H., Brown, R., Jesaitis, A.J., and Parkos, C.A. (1987) The glycoprotein encoded by the X-linked chronic granulomatous disease locus is a component of the neutrophil cytochrome b complex. *Nature* **327**, 717–719
19. Taehan, C., Rowe, P., Parker, P., Totty, N., and Segal, A.W. (1987) The X-linked chronic granulomatous disease gene codes for the β-chain of cytochrome b_{-245}. *Nature* **327**, 720–726
20. Segal, A.W., West, I., Wientjes, F., Nugent, J.H.A., Chavan, A.J., Haley, B., Garcia, R.C., Rosen, H., and Scrace, G. (1992) Cytochrome b_{-245} in a flavocytochrome containing FAD and the NADPH-binding site of the microbicidal oxidase of phagocytes. *Biochem. J.* **284**, 781–788
21. Nisimoto, Y., Otsuka-Murakami, H., and Lambeth, J.D. (1995) Reconstitution of flavin-depleted neutrophil flavocytochrome b_{558} with 8-mercapto-FAD and characterization of the flavin-reconstituted enzyme. *J. Biol. Chem.* **270**, 16428–16434
22. Cross, A.R. and Curnutte, J.T. (1995) The cytosolic activating factors p47*phox* and p67*phox* have distinct roles in the regulation of electron flow in NADPH oxidase. *J. Biol. Chem.* **270**, 6543–6548
23. Yu, L., Quinn, M.T., Cross, A.R., and Dinauer, M.C. (1998) Gp91*phox* is the heme binding subunit of the superoxide-generating NADPH oxidase. *Proc. Natl. Acad. Sci. USA* **95**, 7993–7998
24. Koshkin, V. and Pick, E. (1994) Superoxide production by cytochrome b_{559}. Mechanism of cytosol-independent activation. *FEBS Lett.* **328**, 285–289
25. Doussiere, J., Buzunet, G., and Vignais, P.V. (1995) Photoaffinity labeling and photoinactivation of the O_2^--generating oxidase of neutrophils by an azido derivative of FAD. *Biochemistry* **34**, 1760–1770
26. Rotrosen, D., Yeung, C.L., Leto, T.L., Malech, H.L., and Kwong, C.H. (1992) Cytochrome b_{558}: the flavin-binding component of the phagocyte NADPH oxidase. *Science* **256**, 1459–1462
27. Sumimoto, H., Sakamoto, N., Nozaki, M., Sasaki, H., Takeshige, K., and Minakami, S. (1992) Cytochrome b_{558}, a component of the phagocyte NADPH oxidase, is a flavoprotein. *Biochem. Biophys. Res. Commun.* **186**, 1368–1375
28. Yoshida, L.S., Saruta, F., Hikawa, Y., Tatsuzawa, O., and Tsunawaki, S. (1998) Mutation at histidine 338 of gp91*phox* deletes FAD and affects expression of cytochrome b_{558} of the human NADPH oxidase. *J. Biol. Chem.* **273**, 27879–27886
29. Ravel, P. and Lederer, F. (1993) Affinity-labeling of an NADPH-binding site on the heavy subunit of flavocytochrome b_{558} in particulate NADPH oxidase from activated human neutrophils. *Biochem. Biophys. Res. Commun.* **196**, 543–552
30. Doussiere, J., Brandolin, G., Derrien, V., and Vignais, P.V. (1993) Critical assessment of the presence of an NADPH binding site on neutrophil cytochrome b_{558} by photoaffinity and immunochemical labeling. *Biochemistry* **32**, 8880–8887
31. Smith, R.M., Connor, J.A., Chen, L.M., and Babior, B.M. (1996) The cytosolic subunit p67*phox* contains an NADPH-binding site that participates in catalysis by the leukocyte NADPH oxidase. *J. Clin. Invest.* **98**, 977–983
32. Dang, P.M.C., Babior, B.M., and Smith, R.M. (1999) NADPH

dehydrogenase activity of p67*phox*, a cytosolic subunit of the leukocyte NADPH oxidase. *Biochemistry* **38**, 5746–5753
33. Dang, P.M.C., Johnson, J.L., and Babior, B.M. (2000) Binding of nicotinamide adenine dinucleotide phosphate to the tetratricopeptide repeat domains at the N-terminus of p67*phox*, a subunit of the leukocite nicotinamide adenine dinucleotide phosphate oxidase. *Biochemistry* **39**, 3069–3075
34. Freeman, J.R. and Lambeth, J.D. (1996) NADPH oxidase activity is independent of p47*phox* in vitro. *J. Biol. Chem.* **271**, 22578–22582
35. Koshkin, V., Lotan, O., and Pick, E. (1996) The cytosolic component p47*phox* is not a sine qua non participant in the activation of NADPH oxidase but is required for optimal superoxide production. *J. Biol. Chem.* **271**, 30326–30329
36. Han, C.-H., Freeman, J.R., Lee, J.R., Motalebi, S.A., and Lambeth, J.D. (1998) Regulation of the neutrophil respiratory burst oxidase. Identification of an activation domain in p67*phox*. *J. Biol. Chem.* **273**, 16663–16668
37. Uhlinger, D.J., Tyagi, S.R., Inge, K.L., and Lambeth, J.D. (1993) The respiratory burst oxidase of human neutrophils. Guanine nucleotides and arachidonate regulate the assembly of a multicomponent complex in a semirecombinant cell-free system. *J. Biol. Chem.* **268**, 8624–8631
38. Uhlinger, D.J., Taylor, K., and Lambeth, J.D. (1994) p67*phox* enhances the binding of p47*phox* to the human neutrophil respiratory oxidase complex. *J. Biol. Chem.* **269**, 22095–22098
39. Kreck, M.L., Uhlinger, D.J., Tyagi, S.R., Inge, K.L., and Lambeth, J.D. (1994) Participation of the small molecular weight GTP-binding protein Rac1 in cell-free activation and assembly of the respiratory burst oxidase. *J. Biol. Chem.* **269**, 4161–4168
40. Gentz, R., Chen, C.-H., and Rosen, C.A. (1989) Bioassay for trans-activation using purified human immunodeficiency virus tat-encoded protein: trans-activation requires mRNA synthesis. *Proc. Natl. Acad. Sci. USA* **86**, 821–824
41. Bradford, M. (1976) A rapid and sensitive method for the quantitation of microgram quantities of protein utilizing the principle of protein-dye binding. *Anal. Biochem.* **72**, 248–254
42. Ragan, C.I. and Bloxham, D.P. (1977) Specific labelling of a constituent polypeptide of bovine heart mitochondrial reduced nicotinamide-adenine dinucleotide-ubiquinone reductase by the inhibitor diphenylene iodonium. *Biochem. J.* **163**, 605–615
43. Mitchell, J.A., Kolhaas, K.L., Matsumoto, T., Pollock, J.S., Forstermann, U., Warner, T.D., Schmidt, H.H., and Murad, F. (1992) Induction of NADPH-dependent diaphorase and nitric oxide synthase activity in smooth muscle and cultured macrophages. *Mol. Pharmacol.* **41**, 1163–1168
44. Nomanbhoy, T.K. and Cerione, R.A. (1996) Characterization of the interaction between RhoGDI and Cdc42Hs using fluorescence spectroscopy. *J. Biol. Chem.* **271**, 10004–10009
45. LaVallie, E.R., DiBlasio, E.A., Kovacic, S., Grant, K.L., Schendel, P.F., and McCoy, J.M. (1993) Induction of NADPH-dependent diaphorase and nitric oxide synthase activity in aortic smooth muscle and cultured macrophages. *Bio/Technology* **11**, 187–193
46. Cross, A.R. and Jones, O.T.G. (1986) The effect of the inhibitor diphenylene iodonium on the superoxide-generating system of neutrophils. Specific labelling of a component polypeptide of the oxidase. *Biochem. J.* **237**, 111–116
47. Taylor, W.R., Jones, D.T., and Segal, A.W. (1993) A structural model for the nucleotide binding domains of the flavocytochrome b_{-245} beta-chain. *Protein Sci.* **2**, 1675–1685
48. Nishida, H., Inaka, K., and Miki, K. (1995) Specific arrangement of three amino acid residues for flavin-binding barrel structures in NADH-cytochrome b_5 reductase and the other flavin-dependent reductases. *FEBS Lett.* **361**, 97–100
49. Zhou, Y., Lin, G., and Murtaugh, M.P. (1995) Interleukin-4 suppresses the expression of macrophage NADPH oxidase heavy subunit (gp91*phox*). *Biochim. Biophys. Acta* **1265**, 40–48
50. Bjorgvinsdottir, H., Ling, Z., and Dinauer, M.C. (1996) Cloning of murine gp91*phox* cDNA and functional expression in a human X-linked chronic granulomatous disease cell line. *Blood* **87**, 2005–2010
51. Koshkin, V., Lotan, O., and Pick, E. (1997) Electron transfer in the superoxide-generating NADPH oxidase complex reconstituted in vitro. *Biochim. Biophys. Acta* **1319**, 139–146
52. Cross, A.R., Yarchover, J.L., and Curnutte, J.T. (1994) The superoxide-generating system of human neutrophils possesses a novel diaphorase activity. Evidence for distinct regulation of electron flow within NADPH oxidase by p67*phox* and p47*phox*. *J. Biol. Chem.* **269**, 21448–21454
53. Nisimoto, Y., Motalebi, S.A., Han, C.-H., and Lambeth, J.D. (1999) The p67*phox* activation domain regulates electron flow from NADPH to flavin in flavocytochrome b_{558}. *J. Biol. Chem.* **274**, 22999–23005
54. Uhlinger, D.J., Tyagi, S.R., and Lambeth, J.D. (1995) On the mechanism of inhibition of the neutrophil respiratory burst oxidase by a peptide from the C-terminus of the large subunit of cytochrome b_{558}. *Biochemistry* **34**, 524–527
55. Zhen, L., Yu, L., and Dinauer, M.C. (1998) Probing the role of the carboxyl terminus of the gp91*phox* subunit of neutrophil flavocytochrome b_{558} using site-directed mutagenesis. *J. Biol. Chem.* **273**, 6575–6581
56. Klienberg, M.E., Malech, H.L., Mital, D.A., and Leto, T.L. (1994) p21rac does not participate in the early interaction between p47*phox* and cytochrome b_{558} that leads to phagocyte NADPH oxidase activation in vitro. *Biochemistry* **33**, 2490–2495
57. Biberstine-Kinkade, K.J., Yu, L., and Dinauer, M.C. (1999) Mutagenesis of an arginine- and lysine-rich domain in the gp91*phox* subunit of the phagocyte NADPH oxidase flavocytochrome b_{558}. *J. Biol. Chem.* **274**, 10451–10457
58. Nisimoto, Y., Freeman, J.R., Motalebi, S.A., Hirshberg, M., and Lambeth, J.D. (1997) Rac binding to p67*phox*. Structural basis for interactions of the Rac1 effector region and insert region with components of the respiratory burst oxidase. *J. Biol. Chem.* **272**, 18834–18841
59. Freeman, J.R., Abo, A., and Lambeth, J.D. (1996) Rac "insert region" is a novel effector region that is implicated in the activation of NADPH oxidase, but not PAK65. *J. Biol. Chem.* **271**, 19794–19801
60. Lambeth, J.D., Burnham, D.N., and Tyagi, S.R. (1988) Sphinganine effects on chemoattractant-induced diacylglycerol generation, calcium fluxes, superoxide production, and on cell viability in the human neutrophil. Delivery of sphinganine with bovine serum albumin minimizes cytotoxicity without affecting inhibition of the respiratory burst. *J. Biol. Chem.* **263**, 3818–3822
61. McIver, L., Leadbeater, C., Campopiano, D.J., Baxter, R.L., Daff, S.N., Chapman, S.K., and Munro, A.W. (1998) Characterization of flavodoxin $NADP^+$ oxidoreductase and flavodoxin; key components of electron transfer in *Escherichia coli*. *Eur. J. Biochem.* **257**, 577–585
62. Dewanti, A.R. and Duine, J.A. (1998) Reconstitution of membrane-integrated quinoprotein glucose dehydrogenase apoenzyme with PQQ and the holoenzyme's mechanism of actin. *Biochemistry* **37**, 6810–6818